Received: 13 February 2021 | Revised: 17 April 2021 | Accepted: 18 April 2021

DOI: 10.1111/jnc.15375

ORIGINAL ARTICLE

Journal of Neurochemistry JNC The Official Journal of the International Society for Neurochemistry WILEY

Single intracerebroventricular progranulin injection adversely affects the blood–brain barrier in experimental traumatic brain injury

Regina Hummel[1] | Manuel Lang[1] | Simona Walderbach[1] | Yong Wang[1] | Irmgard Tegeder[2] | Christina Gölz[1] | Michael K. E. Schäfer[1,3,4]

[1]Department of Anesthesiology, University Medical Center of the Johannes Gutenberg-University Mainz, Mainz, Germany

[2]Institute of Clinical Pharmacology, Medical Faculty, Goethe-University Frankfurt, Frankfurt, Germany

[3]Focus Program Translational Neurosciences (FTN) of the Johannes Gutenberg-University Mainz, Mainz, Germany

[4]Research Center for Immunotherapy (FZI) of the Johannes Gutenberg-University Mainz, Mainz, Germany

Correspondence
Michael K. E. Schäfer, Department of Anesthesiology and Focus Program Translational Neurosciences, University Medical Center of the Johannes Gutenberg-University Mainz, Langenbeckstraße 1 (Bld. 505), 55131 Mainz, Germany.
Email: Michael.Schaefer@unimedizin-mainz.de

Funding information
This study was supported by the Mainz Research School of Translational Biomedicine (TransMed) of the University Medical Center, Johannes Gutenberg-University Mainz, Germany, and by the Deutsche Forschungsgemeinschaft (SCHA1261/4-3 to MKES and CRC1080, C02 to IT).

Abstract

Progranulin (PGRN) is a neurotrophic and anti-inflammatory factor with protective effects in animal models of ischemic stroke, subarachnoid hemorrhage, and traumatic brain injury (TBI). Administration of recombinant (r) PGRN prevents exaggerated brain pathology after TBI in *Grn*-deficient mice, suggesting that local injection of recombinant progranulin (rPGRN) provides therapeutic benefit in the acute phase of TBI. To test this hypothesis, we subjected adult male C57Bl/6N mice to the controlled cortical impact model of TBI, administered a single dose of rPGRN intracerebroventricularly (ICV) shortly before the injury, and examined behavioral and biological effects up to 5 days post injury (dpi). The anti-inflammatory bioactivity of rPGRN was confirmed by its capability to inhibit the inflammation-induced hypertrophy of murine primary microglia and astrocytes in vitro. In C57Bl/6N mice, however, ICV administration of rPGRN failed to attenuate behavioral deficits over the 5-day observation period. (Immuno)histological gene and protein expression analyses at 5 dpi did not reveal a therapeutic benefit in terms of brain injury size, brain inflammation, glia activation, cell numbers in neurogenic niches, and neuronal damage. Instead, we observed a failure of TBI-induced mRNA upregulation of the tight junction protein occludin and increased extravasation of serum immunoglobulin G into the brain parenchyma at 5 dpi. In conclusion, single ICV administration of rPGRN had not the expected protective effects in the acute phase of murine TBI, but appeared to cause an aggravation of blood–brain barrier disruption. The data raise questions about putative PGRN-boosting approaches in other types of brain injuries and disease.

Abbreviations: (S) BDPs, (spectrin) breakdown products; BBB, blood–brain barrier; CCI, controlled cortical impact; CNS, central nervous system; Ctsl, cathepsin L; DCX, doublecortin; dpi, days post injury; GAPDH, glyceraldehyde 3-phosphate dehydrogenase; GFAP, glial fibrillary acidic protein; Iba1, ionized calcium-binding adapter molecule 1; ICV, intracerebroventricular; IgG, immunoglobulin G; Il1b, interleukin 1 beta; IR, immunoreactive; LPS, lipopolysaccharide; Mmp9, matrix metallopeptidase 9; NSS, Neurological Severity Score; Ocln, occludin; PBS, phosphate-buffered saline; PDL, poly-D-lysine; PFA, paraformaldehyde; rPGRN, recombinant progranulin; RR, RotaRod; RRID, Research Resource Identifier (see scicrunch.org); SerpinA3N, serpin peptidase inhibitor A3N; SGZ, subgranular zone of the dentate gyrus; Slpi, secretory leukocyte protease inhibitor; TBI, traumatic brain injury; TNFα, tumor necrosis factor alpha; TSPO, 18-kDa translocator protein.

Manuel Lang and Simona Walderbach contributed equally to this work.

KEYWORDS
blood-brain barrier, neuroinflammation, neuroprotection, progranulin, traumatic brain injury

1 | INTRODUCTION

Traumatic brain injury (TBI) is a major cause of death, and survivors often suffer on lifelong consequences (Stocchetti & Zanier, 2016). The primary injury causes multifactorial secondary events including a rapid inflammatory response predominantly driven by brain-resident microglia, astrocytes, and infiltrating peripheral immune cells. Together, these cells create a highly inflammatory microenvironment at lesion sites, which is required for the removal of necrotic tissue and formation of the glial scar (Schäfer & Tegeder, 2018). However, the injury may also spread to distant locations and result in sustained neuroinflammation, blood–brain barrier (BBB) disruption, axonal pathology, and neurodegeneration that can persist for years after the initial injury (Hay et al., 2015; Johnson et al., 2013; Scott et al., 2018). Consequently, TBI patients have an increased risk to develop various comorbidities including chronic neurodegenerative diseases such as frontotemporal dementia (LoBue et al., 2016), Alzheimer's disease or Parkinson's disease (Crane et al., 2016; Faden & Loane, 2015). In particular, the identification of gene mutations that cause chronic neurodegenerative diseases and functional characterization of their non-mutated gene products have revealed potential therapeutic targets in TBI. Among them is the soluble glycoprotein progranulin (PGRN), encoded by the *GRN* gene that is mutated in patients with frontotemporal dementia and certain subtypes of neuronal lipofuscinosis (Hsiung & Feldman, 1993). PGRN is a neuroprotective and anti-inflammatory factor involved in various neuropathological and inflammatory disease conditions (Bateman et al., 2018; Chitramuthu et al., 2017). In the brain, PGRN is primarily synthesized in neurons and upregulated in microglia following injury (Petkau et al., 2010). Studies in PGRN-deficient mice found that endogenous PGRN is a brain protective factor that prevents exaggerated axonal injury, astrogliosis, microgliosis, and BBB damage in response to experimental TBI (Menzel et al., 2017; Tanaka et al.,. ,,2013, 2014). Similar results were reported in PGRN-deficient or PGRN knockdown mouse models of stroke (Jackman et al., 2013b; Kanazawa et al., 2015; Li et al., 2020), spinal cord injury (Wang et al., 2019), or sciatic nerve injury (Altmann et al., 2016). Thus, neuroprotective actions of endogenous PGRN have been demonstrated in various types of acute nervous system injuries. In addition, transgenic mice overexpressing PGRN showed reduced cerebral infarction volume and improved neurological recovery after ischemic stroke (Tao et al., 2012) or sciatic nerve injury (Altmann et al., 2016). These results suggest that administration of PGRN is protective. Along this line, single intracerebroventricular (ICV) administration of recombinant PGRN (rPGRN) attenuated brain pathology after TBI in PGRN-deficient mice (Menzel et al., 2017), after subarachnoid hemorrhage in rats (Li et al., 2015; Zhou et al., 2015), and after ischemia–reperfusion injury in mice (Egashira et al., 2013). Overall, several studies have characterized endogenous and exogenous PGRN as a beneficial factor of therapeutic value in various rodent brain injury models. However, the therapeutic value of rPGRN following experimental TBI in genetically unmodified animals is still elusive.

To this end, we subjected adult male C57Bl/6N mice to the controlled cortical impact (CCI) model of TBI. The observation time was set to 5 days post injury (dpi) to cover the acute phase of TBI. Post-injury analyses included the monitoring of neurological deficits and motor performance over 5 days, followed by brain (immuno)histopathology and gene and protein expression analyses at 5 dpi.

2 | MATERIALS AND METHODS

2.1 | Primary mixed glial cultures

Primary mixed glial cultures were prepared from cerebral cortices of newborn C57BL6 mouse pups (two mouse pup cortices per 25 cm^2 tissue culture flask at postnatal day 1 or 2 sacrificed by decapitation) as described (Menzel et al., 2017; Schildge et al., 2013), and cells were dissociated using the Neural Tissue Dissociation Kit (Miltenyi Biotec). The cells were cultivated in Dulbecco's Modified Eagle Medium (DMEM, 10% fetal calf serum, 1% penicillin/streptomycin) on poly-D-lysine (0.1 mg/ml)-coated culture flasks (Greiner). Mixed glial cultures were maintained for 12 days. Next, 2×10^5 cells/mL were seeded on poly-D-lysine-coated coverslips (0.1 mg/ml), maintained for 48 hr, and treated with lipopolysaccharide (LPS, 100 ng/ml; Sigma-Aldrich), and/or recombinant mouse PGRN (500 ng/ml, R&D Systems) for 16 hr and processed for immunocytochemistry and fluorescence microscopy. Briefly, cells were fixed with 4% paraformaldehyde (PFA) for 20 min and stained with rabbit anti-ionized calcium-binding adapter molecule 1 (Iba1), 1:500; WAKO, Research Resource Identifier, RRID:AB_839504) and rat anti-glial fibrillary acidic protein (GFAP), 1:500; DAKO, RRID:AB_10013382) overnight at 4°C. After incubation with fluorophore-conjugated antibodies (goat anti-rabbit al488, RRID:AB_2576217, goat anti-rat al568, RRID:AB_2534121, 1:1,000; Thermo Fisher) images were taken using a confocal microscope (LSM5 Exciter; Zeiss) with equal acquisition parameters. Morphological parameters of single cells were analyzed using ImageJ (NIH Image, RRID:SCR_003070) and appropriate threshold settings. Independent cell culture preparations were performed ($n = 3$ for microglia, $n = 5$ for astrocytes), and individual cells were examined in each condition ($n \geq 55$ for microglia, $n \geq 297$ for astrocytes).

2.2 | Mice

Male C57BL6/N mice (Janvier, ~22 g, 6–7 weeks old) were housed individually and maintained in a controlled environment (12-hr dark/light cycle, 23°C, 55% humidity) with food and water ad libitum. All

experiments were conducted in compliance with the institutional guidelines of the Johannes Gutenberg University, Mainz, Germany, and approved by the Animal Care and Ethics Committee of the Landesuntersuchungsamt Rheinland-Pfalz (Tierversuchsantrag protocol number G12-1-052). Mice were randomized using a web-based random group generator (www.pubmed.de/tools/zufallsgenerator). Data acquisition and analyses were blinded to the experimenter. Two cohorts of rPGRN/control mice were subjected to experimental CCI and ICV of rPGRN/vehicle followed by assessment of neurological and physiological parameters. The groups were in Cohort 1: CCI vehicle $n = 10$, CCI rPGRN $n = 10$, sham vehicle $n = 5$, sham rPGRN $n = 5$ and in Cohort 2: CCI vehicle $n = 12$, CCI rPGRN $n = 12$, sham vehicle $n = 8$, sham rPGRN $n = 8$. Cohorts were pooled for behavioral analyses and subdivided for (immuno)histochemical stainings (see Table 1 and respective figures). This experimental and exploratory animal study was not preregistered. The required sample size of the CCI groups was based on the assumption that a change in 20% in the brain lesion as a main outcome factor is relevant (e.g., anticipated means 23 mm^3 versus. 28 ± 4 mm^3 standard deviation). The probability of Type I error was set to $\alpha = 0.05$, and the standard statistical power was set to $1 - \beta = 0.8$ (80%), resulting in $\beta = 0.2$ (probability of Type II error).

2.3 | Surgical procedures

Experimental TBI was performed during daytime using the CCI model essentially as described (Hummel et al., 2020). Briefly, animals were anesthetized with isoflurane inhalation (induction 4%, maintenance 2.1% (v/v)) to ensure sufficient anesthesia during the whole procedure. Mice were fixed to a stereotactic apparatus (Kopf Instruments), rectal temperature was maintained at 37°C with a feedback-controlled heating pad (Hugo Sachs, March-Hugstetten, Germany), and a small burr hole was drilled for ICV injection. ICV injection of recombinant mouse progranulin (rPGRN; R&D Systems) or vehicle (phosphate-buffered saline [PBS]) was performed shortly before CCI. rPGRN was injected into the ipsilateral ventricle using a Hamilton syringe placed to the stereotactical coordinates: anteroposterior −0.5 mm, lateral from bregma +1 mm, and ventral from dura −1.6 mm. The syringe was hold in place for 2 min before and 5 min after injection. A total volume of 4 µl (1 µg rPGRN in PBS) was injected per 2 µl/min. After midline incision and craniotomy, CCI was induced above the right parietal cortex with an electromagnetically controlled stereotaxic impactor (Leica Biosystems, Impact One; velocity: 6 m/s; duration: 200 ms; impact depth: 1.5 mm). The post-TBI observation time was 5 dpi. Sham mice were treated equally to CCI mice in terms of anesthesia, skin incision, wound closure, and ICV injection with PBS or rPGRN but without craniotomy. Craniotomy itself can contribute to brain damage in our TBI model (Cole et al., 2011). Therefore, only light non-penetrating drilling on the bone surface was performed to allow comparisons between non-injured and injured brains (Krämer et al., 2017). Criteria for postoperative analgesic treatment were predefined and included exhibiting signs of severe pain or discomfort (e.g., aggression, piloerection, hunched posture, or autonomous reactions like rapid, shallow breathing) in accordance with national and international recommendations, and animals were correspondingly screened several times daily. No animals in the CCI or sham groups, however, needed postoperative analgesic treatment. This is in line with a recent study that shows that CCI causes only minor signs of pain and stress (Staib-Lasarzik et al., 2019). Before and after TBI, the neurobehavioral outcome of mice was daily assessed using a neurological severity score (NSS) as described (Hummel et al., 2020). Mouse performance was tested in nine different tasks pre-injury and at 1, 3, and 5 dpi to evaluate the motor ability, alertness, balancing, and general behavior (severe neurological dysfunction NSS = 12; Figure 2a). Three experimenters did the experiments, all in a blinded manner, one performing the sham or CCI procedure, one performing drug or vehicle application, and the third performing behavioral analyses. All post-interventional analyses were performed in a blinded and unbiased fashion.

TABLE 1 Group allocation and animal numbers

	CCI vehicle	CCI rPGRN	Sham vehicle	Sham rPGRN
NSS and weight	$n = 22$	$n = 22$	$n = 13$	$n = 13$
Brain lesion volume	$n = 16$	$n = 16$	-	-
Gene expression analysis	$n = 16$	$n = 16$	$n = 9$	$n = 9$
Protein analysis	$n = 16$	$n = 16$	$n = 9$	$n = 9$
IHC (Iba1/GFAP, DCX/Ki−67 vibratome sections)	$n = 6$	$n = 6$	$n = 4$	$n = 4$
IHC (IgG, cryotome sections)	$n = 10$	$n = 10$	–	–

Abbreviations: CCI, controlled cortical impact; DCX, doublecortin; GFAP, glial fibrillary acidic protein; IgG, immunoglobulin G; rPGRN, recombinant progranulin.

2.4 | (Immuno)histology

Mice were anesthetized with 4 vol% isoflurane, decapitated, and brains were dissected, immediately frozen in powdered dry ice and stored at −20°C. Cryostat brain sectioning (HM 560 Cryostat; Thermo Scientific) and cresyl violet staining were carried out as described (Gölz et al., 2019). Brains were cut to 12-µm-thick slices and collected every 500 µm on glass slides (SuperFrost Plus, Thermo Scientific). The quantification of brain lesion volumes was performed as described (Menzel et al., 2017; Schaible et al., 2014). Briefly, 16 coronal sections beginning at bregma +3.14 mm according to the Mouse Brain Library atlas (http://www.mbl.org) each

at a distance of 500 μm were analyzed. The region of damaged brain tissue is defined as the region lacking cresyl violet staining. To calculate the lesion volume, the areas from the 16 sections were multiplied and calculated based on the following formula: 0.5*(A1+A2+...+A16). Brain tissue material containing the lesion or corresponding healthy tissue from sham animals was taken between the sections collected for histological analyses, snap-frozen in liquid nitrogen, and further processed for gene and protein expression analyses.

Digitalization and analysis was carried out in a blinded fashion using a bright-field microscope (Stemi 305, Zeiss) and Zen software (Zeiss, RRID:SCR_013672). For immunohistochemistry, 12-μm frozen sections were air-dried for 30 min, fixed with 4% PFA for 10 min, and blocked in PBS, pH 7.4 containing 5% goat serum, 0.5% bovine serum albumin, and 0.1% Triton X-100. Vibratome sections, 80 μm thick, were fixed in 4% PFA for 1 day and blocked in PBS, pH 7.4 containing 5% goat serum, 0.5% bovine serum albumin, and 0.3% Triton X-100 at room temperature for 2 hr. The following primary and secondary antibodies were used (designation, dilution, supplier, RRID): rabbit anti-Iba1 (1:1,500; Wako, RRID:AB_839504), rat anti-GFAP (1:1,000; Invitrogen, RRID:AB_86543), rat anti-Ki-67 (1:500; eBioscience, RRID:AB_10853185), and guinea pig anti-doublecortin (anti-DCX, 1:500; Merck Chemicals, RRID:AB_1586992). Primary antibodies were diluted in blocking solution and incubated on sections overnight at 4°C. Secondary antibodies (goat anti-rabbit al488, RRID:AB_2576217, goat anti-rat al488 RRID:AB_141373, goat anti-guinea pig al568, RRID:AB_2534119, goat anti-rat al568, RRID:AB_141874, 1:500; Invitrogen/Thermo Fisher) were diluted in blocking solution, and sections were incubated overnight at 4°C. All sections were counterstained with DAPI (1:10.000; Sigma-Aldrich) and mounted in Immu-Mount (Thermo Fisher).

Images of individual immunostainings were captured using equal filter and acquisition parameters to assure comparability independent of experimental conditions with a confocal laser scanning microscope (LSM5 Exciter; Zeiss). The number of GFAP and Iba1 immunoreactive (IR) particles were determined in the perilesional brain tissue. Images were analyzed using ImageJ (NIH Image) with appropriate threshold settings for background subtraction and the particle count plugin (size: GFAP-IR particles: 30–1000 μm^2, Iba1-IR particles: 20–1000 μm^2). Ki-67 and DCX-positive cells were counted by visual inspection of the subgranular layer of the upper blade of the hippocampus. For anti-immunoglobulin G (IgG) immunostaining, cryosections were air-dried, fixed in 4% PFA, and stained with horseradish peroxidase (HRP)-conjugated goat anti-mouse IgG antibody (1:500; Santa Cruz Biotechnology, RRID:AB_631737) for 90 min at room temperature. After digitalization of the images, quantification of the extravasation volume relative to the ipsilesional hemisphere was performed using a bright-field microscope (Stemi 305; Zeiss) and Zen software (Zeiss, RRID:SCR_013672) according to already published protocols (Huang et al., 2016). All analyses were carried out in a blinded fashion.

2.5 | Gene expression analyses

During histological processing of the brains, 30-μm coronal slices at the contusion level (beginning at bregma +3.14 mm) were separated between the left and right hemisphere, and the upper right quadrants containing the lesioned and the perilesional brain tissue were snap-frozen in liquid nitrogen, stored at −80°C, and processed for gene expression analyses as described (Timaru-Kast et al., 2012). RNeasy and QuantiTect Reverse Transcription Kits (Qiagen) were used to extract RNA and to transcribe mRNA to cDNA. Analyses were carried out using SYBR Green Kit or Maxima Hot Start Kit (both Thermo Scientific) with primer and probes from Eurofins by quantitative polymerase chain reaction (qPCR) (LightCycler 480; Roche). All values were normalized to the housekeeping gene cyclophilin A (*Ppia*), and absolute quantification was performed using a gene specific standard curve of mRNA copies (Thal et al., 2008). For sequences of applied oligonucleotide primer pairs (5′–3′) see Table 2.

2.6 | Immunoblotting

Brain tissue sections at perilesional sites were collected during histological sectioning and processed for immunoblotting essentially as described (Gölz et al., 2019). Briefly, tissue sections were homogenized in ice-cold RIPA lysis buffer [composition: 50 mM Tris-HCl, pH 7.5, 150 mM NaCl, 1 mM EDTA, 1% (v/v) NP-40, 0.1% (v/v) sodium dodecyl sulfate, complete protease inhibitors (Roche)], and protein concentrations were determined and equal amounts of proteins (50 μg per sample) were separated by SDS-PAGE and transferred to nitrocellulose membranes (Perbio Science). The following primary antibodies were used: rabbit anti-GFAP (6F2, 1:2000, Dako, RRID:AB_10013382), mouse anti-αII-spectrin (1:750; Enzo Life Sciences, RRID:AB_10554860) and mouse anti-glyceraldehyde 3-phosphate dehydrogenase (GAPDH), Acris Antibodies, 1:1,000, RRID:AB_1616730) with appropriate species-specific secondary infrared dye-conjugated antibodies (LI-COR, 1:10,000, goat anti-rabbit IgG IRDye 680, RRID:AB_621841; goat anti-mouse IgG IRDye 800, RRID:AB_10793856) to reveal protein band densities using the Odyssey SA Imaging System and quantification with Image Studio (RRID:SCR_014579; LI-COR). To evaluate BBB integrity, proteins lysed in RIPA buffer (2 μl per dot, 2 μg protein each) were spotted onto nitrocellulose membrane, washed 10 min in TBST, and incubated with goat anti-mouse IRdye800 (1:10,000; goat anti-mouse IgG IRDye 800, RRID:AB_10793856) for 1 hr at room temperature. The fluorescence signal was detected using the Odyssey SA Imaging System and quantified with Image Studio.

2.7 | Statistical analysis

Data was analyzed using GraphPad Prism (Versions 7.04 and 8.1, RRID:SCR_002798). All datasets were tested for normal distribution

TABLE 2 Primer sequences for PCR

PCR assay (amplicon size)	Oligonucleotide sequences 5′–3′	Gene bank number
Ppia	fw-GCGTCTSCTTCGAGCTGTT rev-RAAGTCACCACCCTGGCA	NM_008907
Il1b	fw-GTGCTGTCGGACCCATATGAG rev-CAGGAAGACAGGCTTGTGCTC	NM_008361
Tnfa	fw-TCTCATCAGTTCTATGGCCC rev-GGGAGTAGACAAGGTACAAC	NM_008361
Iba1	fw-ATCAACAAGCAATTCCTCGATGA rev-CAGCATTCGCTTCAAGGACATA	NM_019467
Tspo	fw-GCCTACTTTGTACGTGGCGAG rev-CCTCCCAGCTCTTTCCAGAC	NM_009775
Gfap	fw-CGGAGACGCATCACCTCTG rev-TGGAGGAGTCATTCGAGACAA	NM_001131020
SerpinA3N	fw-GCCTCGTCAGGCCAAAAAG rev-TGAACGTGTCAAGAGGGTCAA	NM_009252
Slpi	fw-GTTCCCATTCGCAAACCAG rev-ACTTTCCCACATATACCCTCAC	NM_011414.3
Ctsl	fw-AAGCCATCCGTCTCTCCAGTTC rev-TCCATACCCCATTCACTTCCCC	NM_009984.4
Mmp9	fw-AAGTCTCAGAAGGTGGAT rev-AATAGGCTTTGTCTTGGTA	NM_013599
Grn	fw-ATGCTGTGTGCTGTGAGGAC rev-CACTCCACATTCCCAACCTT	NM_008175
Ocln	Cy5-AGATGCCAGTTGCGGGAGAA fw-GCAAATTATCGCACATCAAGAG fl-GGAGATTATGACAGACGGAAACCTTAG rev-TGTTCAGCCCAGTCAATTATC	NM_008756

Abbreviations: Ctsl, cathepsin L; GFAP, glial fibrillary acidic protein; Il1b, interleukin 1 beta; Mmp9, matrix metallopeptidase 9; NSS, Neurological Severity Score; Ocln, occluding; SerpinA3N, serpin peptidase inhibitor A3N; Slpi, secretory leukocyte protease inhibitor.

using the Shapiro–Wilk test and QQ-plots, and outliers were identified by ROUT test and excluded from further analysis as indicated in the figure legends. Parametric data were statistically analyzed using unpaired Student's *t*-test, and nonparametric data were analyzed using the Mann–Whitney *U*-test with two-sided tests. For multiple groups, one-way ANOVA or Kruskal–Wallis tests with adequate post hoc analyses (Holm–Sidak or Dunn's correction, respectively) were used. Values are expressed individually and as mean ± *SEM*. Tests were considered statistically significant at multiplicity-adjusted p-value < 0.05. Significance levels are indicated by asterisks (*p <.05, **p <.01, ***p <.001, ****p <.0001).

3 | RESULTS

3.1 | rPGRN inhibits the inflammation-induced morphological transition of microglia and astrocytes in vitro

To test the biological activity of rPGRN, murine primary glial cultures were grown for 2 weeks and treated with pro-inflammatory LPS (100 ng/ml) in the presence or absence of rPGRN (500 ng/ml) for 16 hr. In untreated control cultures or in cultures treated with rPGRN alone, double immunostaining for the microglia marker Iba1 or the astrocyte marker GFAP demonstrated a typical "resting" morphology of microglia and a polygonal fibroblast-like shape of astrocytes (Figure 1a). LPS treatment caused marked morphological alterations, that is, an increase in the area of microglia and a shift toward an irregular, stellate shape of astrocytes (Figure 1b). However, the LPS-induced morphological transitions appeared to be less pronounced in the presence of rPGRN (Figure 1c,d). Quantification of microglia area and the relative number of stellate shape astrocytes revealed that rPGRN almost prevented the LPS-induced morphological alterations of microglia and astrocytes (Figure 1e,f). Thus, rPGRN inhibited inflammation-induced morphological transitions of microglia and astrocytes in vitro, confirming its anti-inflammatory biological activity in accordance with previous findings from our and other laboratories (Chiba et al., 2018; Lau et al., 2016; Menzel et al., 2017).

3.2 | Administration of rPGRN does not influence acute neurological deficits or brain lesion size

To test the hypothesis that rPGRN has therapeutic effects in TBI, we subjected C57Bl6 wild-type mice to the CCI model of TBI and administered rPGRN (250 ng/µl in PBS) or vehicle solution (PBS) via

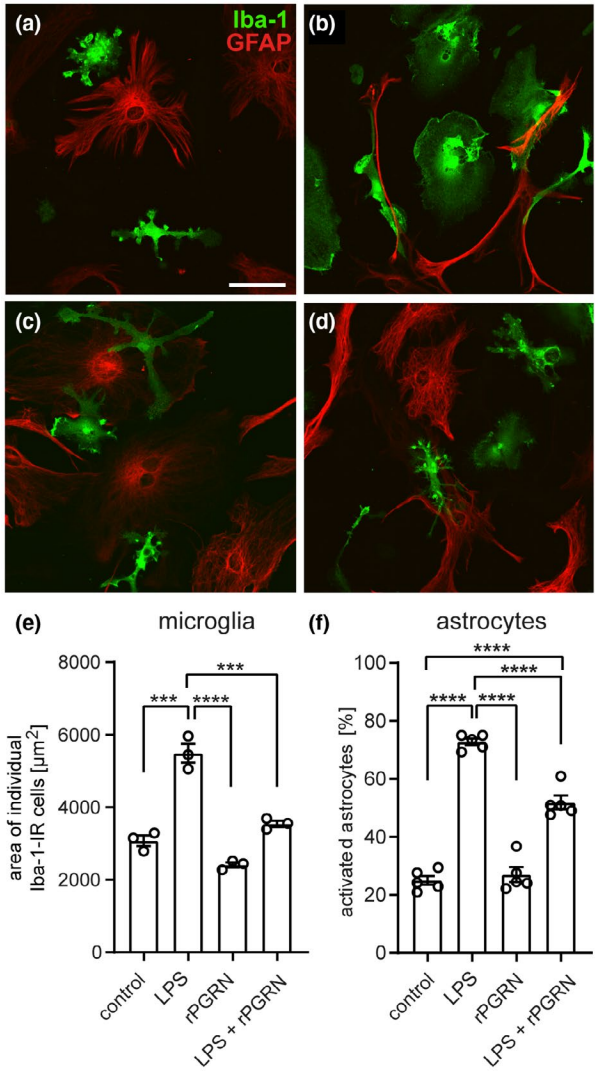

FIGURE 1 Recombinant progranulin (rPGRN) inhibits the inflammation-induced morphological transition of microglia and astrocytes in vitro. (a–d) Double immunofluorescence staining of microglia (anti-Iba1, ionized calcium-binding adapter molecule 1, green) and astrocytes (anti-GFAP, glial fibrillary acidic protein, red). (a, c) Cultures in the absence or presence of rPGRN. Microglia showed a typical "resting" morphology and astrocytes a polygonal fibroblast-like shape. (b,d) Cultures treated with lipopolysaccharide (LPS) in the absence or presence of rPGRN. Microglia and astrocytes showed marked morphological transitions which appeared, however, less pronounced in the presence of rPGRN. (e) Histogram showing the mean area of anti-Iba1-immunostained microglia under different treatment conditions. rPGRN inhibited the LPS-induced increase in area of microglia. (f) Histogram showing the percentage of anti-GFAP-immunostained stellate astrocytes under different treatment conditions. rPGRN attenuated LPS-induced morphological transition from polygonal to stellate astrocytes. Data are expressed as mean ± *SEM*, and individual values are shown, and *p*-values were calculated by ANOVA with Holm–Sidak correction (***$p < .001$, ****$p < .0001$). Scale bar: 200 µm. Sample size: microglia (number of independent cell culture preparations: $n = 3$, at least 55 cells per group); astroglia (number of independent cell culture preparations: $n = 5$, at least 297 cells per group)

ICV to anesthetized animals immediately prior to CCI. The duration of anesthesia and surgery was similar between the experimental groups (sham vehicle: 28.3 ± 0.6 min, sham rPGRN: 29.5 ± 0.7 min, CCI vehicle: 30.9 ± 0.8 min, CCI rPGRN: 30.7 ± 0.7 min, ± *SEM*). Physiological parameters including body temperature during the operation or perioperative body weight of the animals were monitored. While body temperature was unaffected, rPGRN-treated CCI animals showed a trend toward an increased loss of body weight at 1 dpi compared with vehicle (Figure 2b $p = .075$). At 5 dpi, however, the body weights of rPGRN- and vehicle-treated CCI mice were similarly restored. Sham groups gained weight over time regardless of rPGRN treatment (Figure 2b). All mice survived the CCI or sham procedure and the 5 dpi.

Furthermore, assessment of neurological deficits using a composite NSS did not reveal significant differences between rPGRN- and vehicle-treated animals at 1, 3, or 5 dpi (Figure 2c). At 5 dpi, animals were sacrificed, and brains were dissected and processed for cryosectioning, cresyl violet staining, and brain lesion volumetry (Figure 2d). The extent of brain lesion was not statistically different between rPGRN- or vehicle-treated CCI mice. However, rPGRN-treated animals showed a trend toward increased brain damage (Figure 2e $p = .0984$).

3.3 | rPGRN does not alter pro-inflammatory cytokine expression and glia activation after TBI

Our previous work showed that ICV rPGRN treatment in *Grn*-deficient mice prevented the exaggerated brain inflammatory responses to TBI that result from progranulin deficiency (Menzel et al., 2017). To study the effects of rPGRN on brain inflammation in wild-type mice, we examined gene expression regulation of the pro-inflammatory cytokines tumor necrosis factor alpha and IL-1β, the astrocyte activation markers GFAP and serpin peptidase inhibitor A3N (SerpinA3N), and the microglia markers Iba1 and 18-kDa translocator protein at 5 dpi. Both expressions of *Tnfa* and *Il1b* were significantly increased after CCI, but were not influenced by ICV administration of rPGRN (Figure 3a,b). Similar results were obtained for the gene expressions of the microglia markers *Iba1* and *Tspo* as well as the astrocyte markers *Gfap* and *Serpina3n*, which were induced after CCI, but equally in vehicle and rPGRN groups (Figure 3c–f).

To study the local activation of microglia/macrophages and astrocytes at perilesional sites at 5 dpi, we performed immunohistochemistry using antibodies specific to Iba1 or GFAP, respectively (Figure 4a). An increased number of Iba1-IR cells demonstrated brain inflammation after CCI, but no differences were observed between rPGRN- and vehicle-treated CCI animals (Figure 4b). Likewise, the number of GFAP-IR astrocytes was significantly increased after trauma, but the extent of gliosis did not differ between treatment groups (Figure 4c). Hence, single-dose ICV injection of rPGRN did not alter pro-inflammatory cytokine expression and activation of glia after CCI.

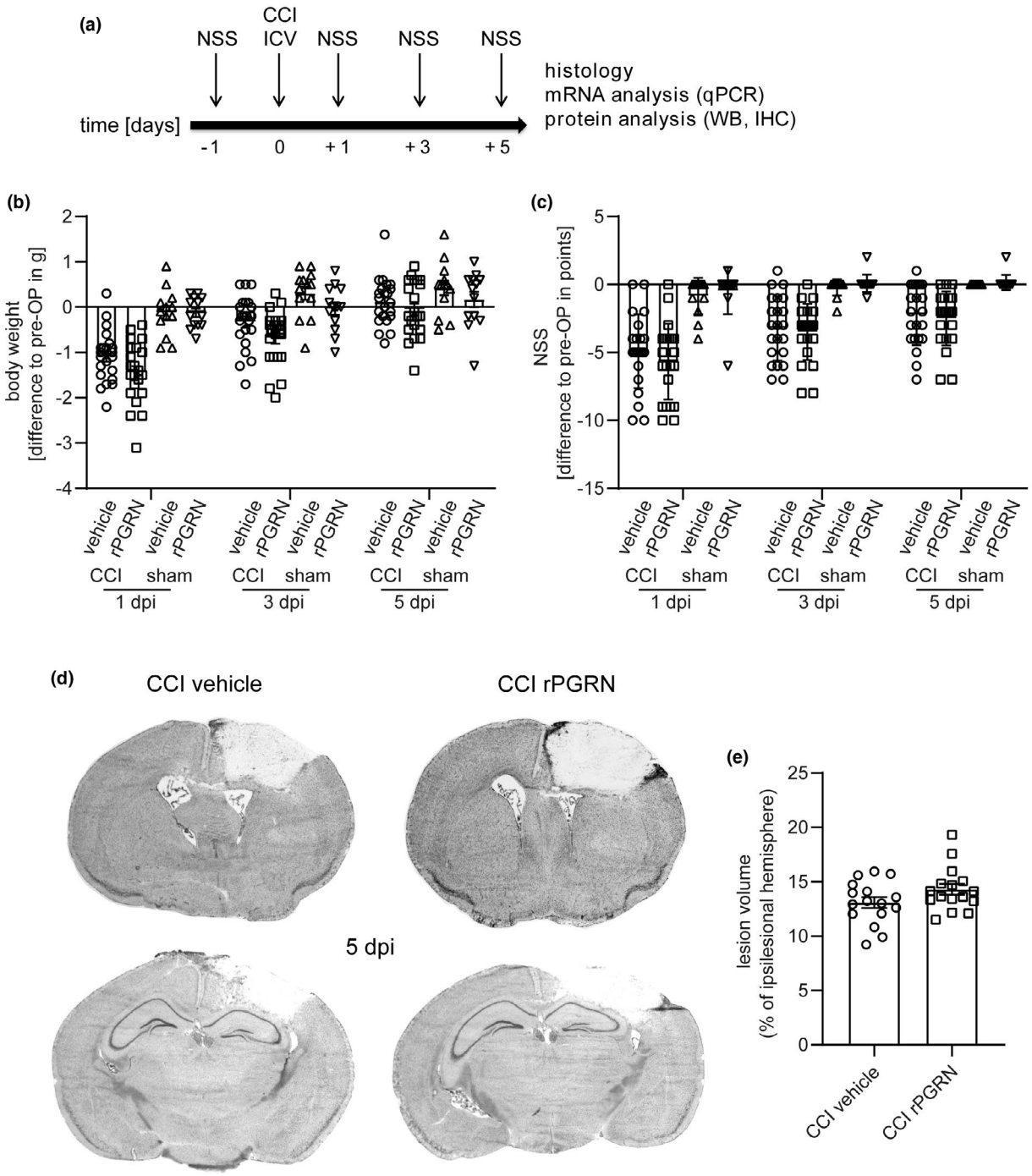

FIGURE 2 Administration of recombinant progranulin (rPGRN) does not influence acute neurological deficits or brain lesion size. (a) Experimental timeline: neurological severity score (NSS) was examined at 1 day before controlled cortical impact (CCI) at 1, 3, and 5 days post injury (dpi). Animals received vehicle or rPGRN intracerebroventricular (ICV) shortly before craniotomy and CCI (or sham procedure). After a survival time of 5 days, brains were processed for histology, mRNA, and protein analyses. (b) Body weight of mice at posttraumatic day 1, 3, and 5 in difference to pre-OP [g]. (c) NSS day 1, 3, and 5 points in difference to the pre-CCI baseline. Sample size NSS/ weight: vehicle CCI: *n* (number of animals) = 22, rPGRN CCI: *n* = 22, vehicle sham: *n* = 13, rPGRN sham: *n* = 13. (d) Representative images of cresyl violet-stained brain sections at two different bregma levels (out of 16) at 5 dpi with vehicle or rPGRN treatment (e) Quantification of lesion volume in % of the ipsilesional hemisphere (vehicle CCI: *n* = 16, rPGRN CCI: *n* = 16). Data points represent individual animals, and data are expressed as mean ± *SEM*. Data was analyzed by one-way ANOVA with Holm–Sidak correction (b), Kruskal–Wallis test with Dunn's correction (c), and unpaired *t*-test (e)

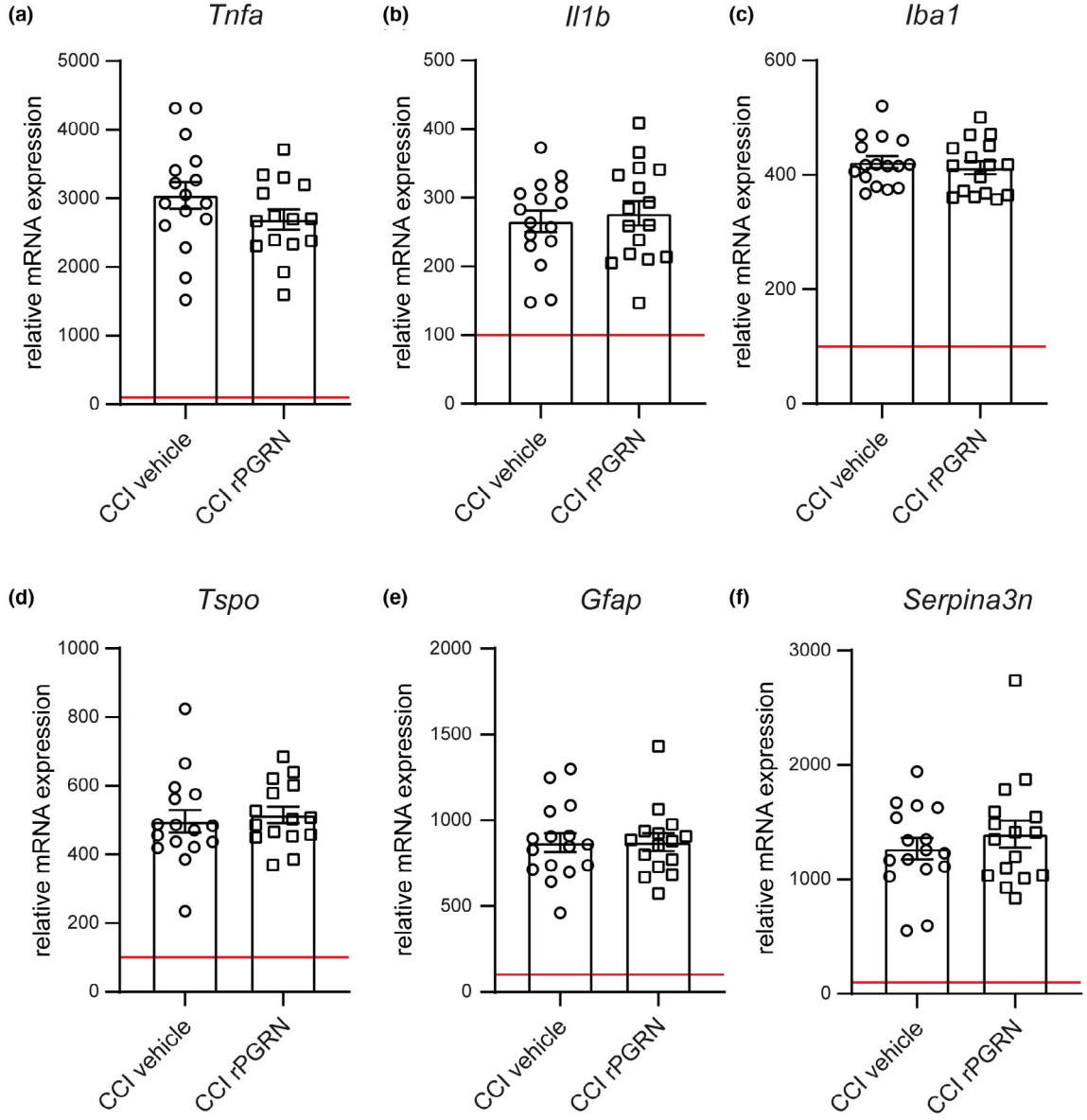

FIGURE 3 Recombinant progranulin (rPGRN) does not alter pro-inflammatory cytokine expression and glia activation after traumatic brain injury. Gene expression analyses of pro-inflammatory and gliosis markers normalized to *Ppia* (sham set to 100% = red line). Quantification of the pro-inflammatory cytokines *Tnfa* (a) and interleukin 1 beta (Il1b) (b), microglia markers *Iba1* (c) and *Tspo* (d) and the astrogliosis markers glial fibrillary acidic protein (*Gfap*) (e) and *Serpina3n* (f). (a–f) Sample size vehicle controlled cortical impact (CCI): *n* (number of animals) = 16, rPGRN CCI: *n* = 16. One significant outlier as determined by ROUT's test was removed from the rPGRN CCI group in (a), (d), and (e). Data are expressed as mean ± *SEM*, and individual values are shown

3.4 | PGRN proteolysis regulatory genes are upregulated after TBI

PGRN is cleaved by various proteases to release individual granulin peptides (Bateman et al., 1990). To assess the interaction of regulatory genes in our TBI model, we analyzed gene expression of enzymes involved in the proteolytic cleavage of PGRN. After CCI, secretory leukocyte protease inhibitor (*Slpi*), *cathepsin L* (*Ctsl*), and *matrix metallopeptidase 9* (*Mmp9*) were upregulated compared with sham animals, but not influenced by rPGRN administration (Figure 5a–c). However, we found that mice that received rPGRN had a reduced *Grn* mRNA expression after CCI (Figure 5d), suggesting a counter-regulatory response that may have obscured putative therapeutic effects.

3.5 | Cell proliferation and the number of immature neurons in neurogenic niches are not affected by rPGRN after TBI

Depending on the severity of the injury, TBI increases or suppresses neurogenesis in the adult hippocampus (Dash et al., 2001; Wang et al., 2016). Previous work indicated that PGRN increases adult hippocampal neurogenesis following voluntary exercise

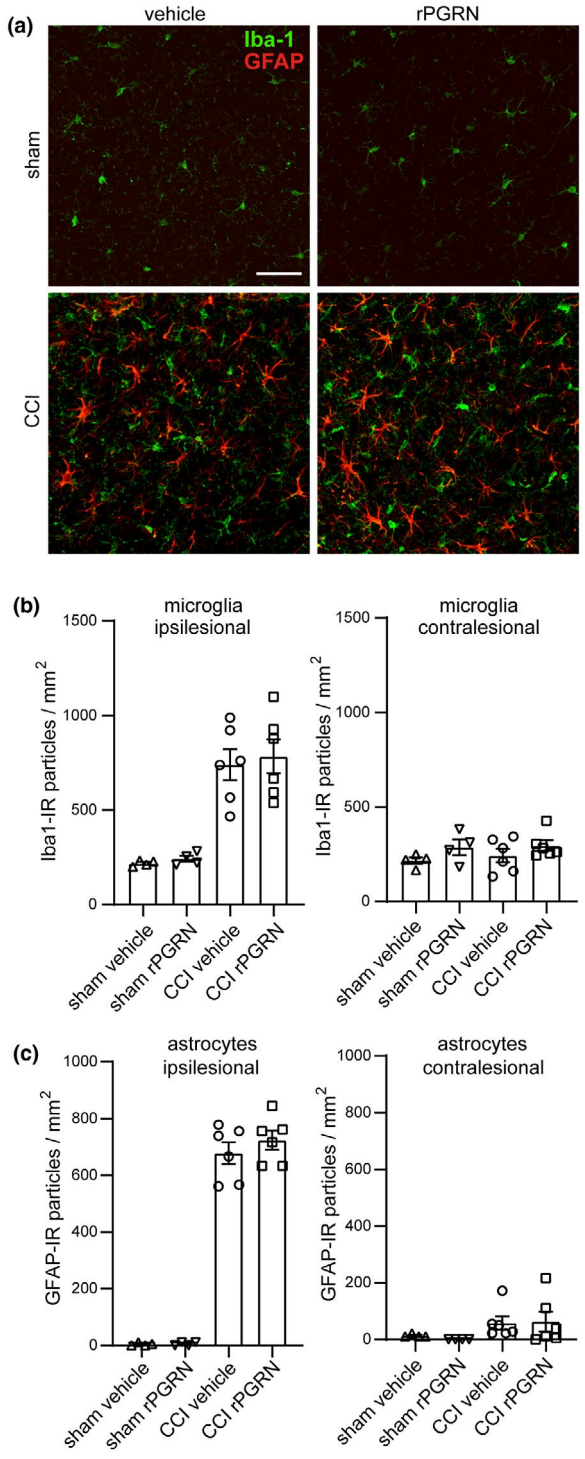

FIGURE 4 Recombinant progranulin (rPGRN) does not have an impact on the activation of microglia/macrophages or the number of astrocytes at perilesional sites. (a) Representative immunofluorescence images of vibratome sections stained for Iba1 (ionized calcium-binding adapter molecule 1) and glial fibrillary acidic protein (GFAP), illustrating distribution and morphology of microglia/macrophages and astrocytes, respectively. Images are taken in the region of the perilesional cortex of the injured hemisphere 5 days after traumatic brain injury. Quantification of Iba1-immunoreactive (IR) cells (b) and GFAP-IR cells (c). Sample size: vehicle controlled cortical impact (CCI): *n* (number of animals) = 6, rPGRN CCI: *n* = 6, vehicle sham: *n* = 4, rPGRN sham: *n* = 4. Data are expressed as mean ± *SEM*, and individual values are shown. Scale bar: 50 μm

(Asakura et al., 2011) and maintains neurogenesis in the presence of excessively activated microglia (Ma et al., 2017). To assess cell proliferation and neurogenesis in neurogenic niches after CCI with/without rPGRN ICV treatment, we examined the subgranular zone of the hippocampal dentate gyrus (Figure 6a) by double immunostaining with antibodies specific for the cell cycle and proliferation marker Ki-67 and the immature neuron marker doublecortin (DCX) (Figure 6b). IR cells in the upper blade of the septal hippocampus were counted in sections from rPGRN- and vehicle-treated animals. While the number of Ki-67-IR cells almost doubled after CCI, the number of DCX IR cells did not change (Figure 6c). However, treatment with rPGRN had no effect on the number of proliferating cells or immature neurons in the hippocampal subgranular zone at 5 dpi.

3.6 | Neuronal injury and astrocyte activation are not influenced by rPGRN

Spectrin breakdown products (SBDPs) serve as indicators of an overall disturbance of intracellular Ca^{2+} homeostasis, excitotoxicity, and neuronal and axonal injury after experimental TBI (Hummel et al., 2020; Newcomb et al., 1997; Schober et al., 2014). Immunoblot analyses revealed an increase of SBDPs of 145/150 kDa owing to calpain and caspase-3 induced spectrin cleavage after CCI (Figure 7a). However, administration of rPGRN did not attenuate or increase the generation of SBDPs compared with vehicle (Figure 7b).

TBI can also lead to mechanical injury of astrocytes and increased posttraumatic reactivity (Zhou et al., 2020). To confirm our findings on GFAP gene expression and perilesional astrocyte reactivity, we investigated GFAP protein levels in ipsilesional and sham brain tissue. Immunoblot analysis showed a marked increase of GFAP protein expression after CCI, but rPGRN treatment did not affect the levels of GFAP (Figure 7c).

3.7 | rPGRN adversely affects the blood–brain barrier after TBI

PGRN has been reported to protect the BBB in a rat model of acute ischemic stroke (Kanazawa et al., 2015). To assess the effect of rPGRN on BBB leakage in our TBI model, extravasated serum IgG levels were analyzed by dot-immunoblot assay. At 5 dpi, brain lysates of ipsilesional hemispheres from vehicle-treated CCI mice contained IgG levels more than five times higher than sham mice. Corresponding brain samples from rPGRN-treated CCI mice, however, contained significantly higher levels of IgG compared with vehicle treatment,

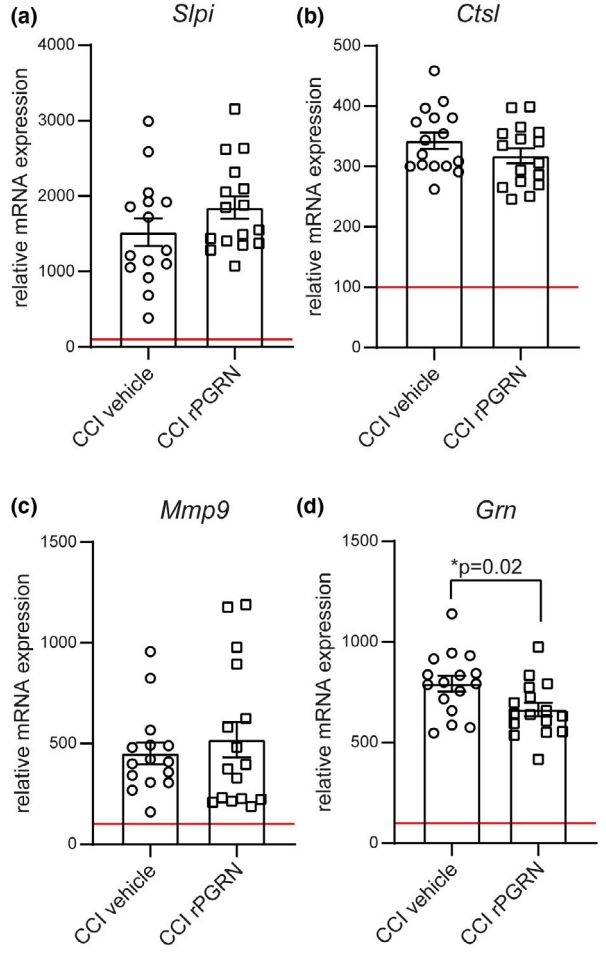

FIGURE 5 Progranulin (PGRN) proteolysis regulatory genes are upregulated after traumatic brain injury. Gene expression normalized to PPIA (sham set to 100% = red line). (a–d): Quantification of the relative mRNA expression of the enzymes secretory leukocyte protease inhibitor secretory leukocyte protease inhibitor (*Slpi*) (a), cathepsin L (*Ctsl*) (b), and matrix metalloprotease 9 (*Mmp9*) (c) as well as gene expression of *Grn* (d). Sample size: vehicle controlled cortical impact (CCI): *n* (number of animals) = 16, rPGRN (recombinant PGRN) CCI: *n* = 16. One significant outlier as determined by ROUT's test was removed from the rPGRN CCI group in (a) and (c). Data are expressed as mean ± *SEM* with individual values, and *p*-values were calculated by unpaired *t*-test (*$p < .05$)

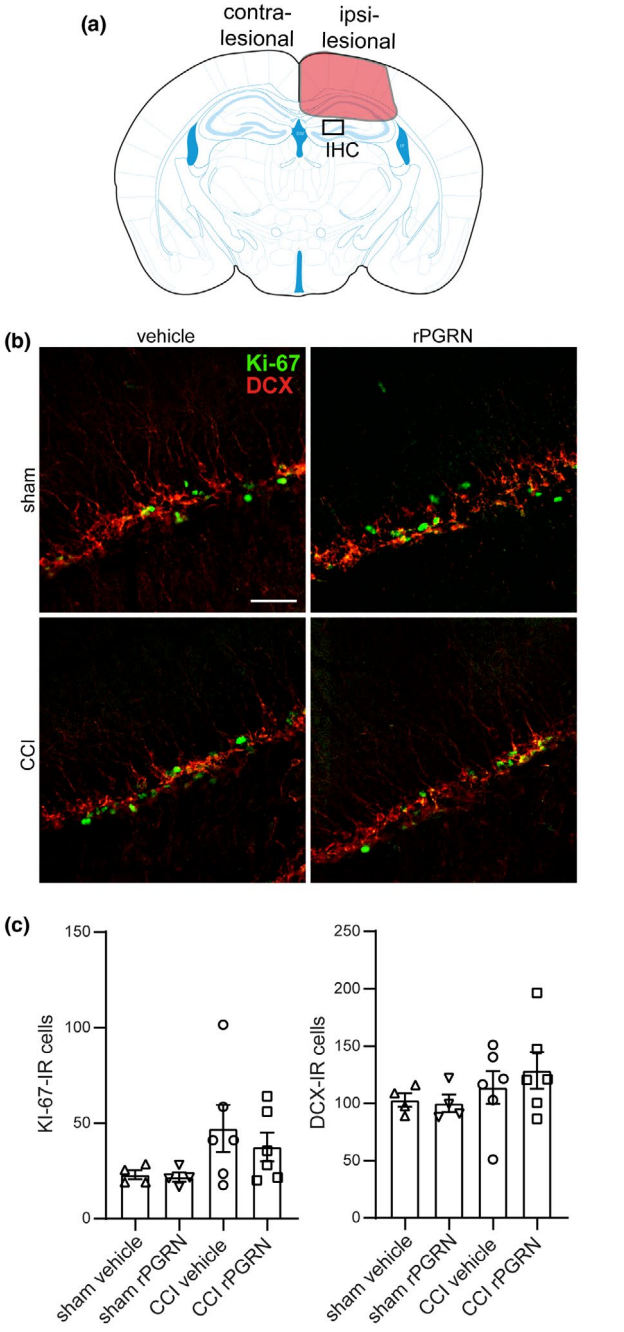

FIGURE 6 Cell proliferation and the number of immature neurons in neurogenic niches are not affected by recombinant progranulin (rPGRN) after traumatic brain injury. (a) Scheme showing the lesion core (red) and the region of interest for the examination of cell proliferation and of immature neurons by anti-Ki67 and anti-doublecortin (DCX) immunohistochemistry (IHC, black box). (b) Representative images of vehicle- and rPGRN-treated sham and controlled cortical impact (CCI) animals at 5 dpi. (c) Quantification of Ki-67 and DCX immunoreactive (IR) cells. Sample size: vehicle CCI: *n* (number of animals) = 6, rPGRN CCI: *n* = 6, vehicle sham: *n* = 4, rPGRN sham: *n* = 4. Data represent mean ± *SEM* with individual values. Scale bar: 50 μm

suggesting exacerbated BBB damage (Figure 8a,b). To substantiate this result, brain sections were immunostained with anti-IgG, and the extent of IgG extravasation was determined. IgG extravasation was apparent as a diffuse staining in the perilesional brain parenchyma. In agreement with the result from the dot immunoblot, the area of IgG extravasation in brain sections of rPGRN-treated compared with vehicle-treated CCI mice was increased by 12% (Figure 8d,e).

Tight junctions are an important component of the BBB and considered sensitive indicators of normal and impaired functional states of the BBB (Almutairi et al., 2016). Regulation of the tight junction protein occludin has been shown at both the mRNA and protein level in animal models of stroke (Jiao et al., 2011) or TBI (Wen et al., 2014). Therefore, we examined gene expression levels of occludin to assess the molecular integrity of the BBB. Occludin mRNA expression was increased in ipsilesional brain samples from vehicle-treated CCI mice

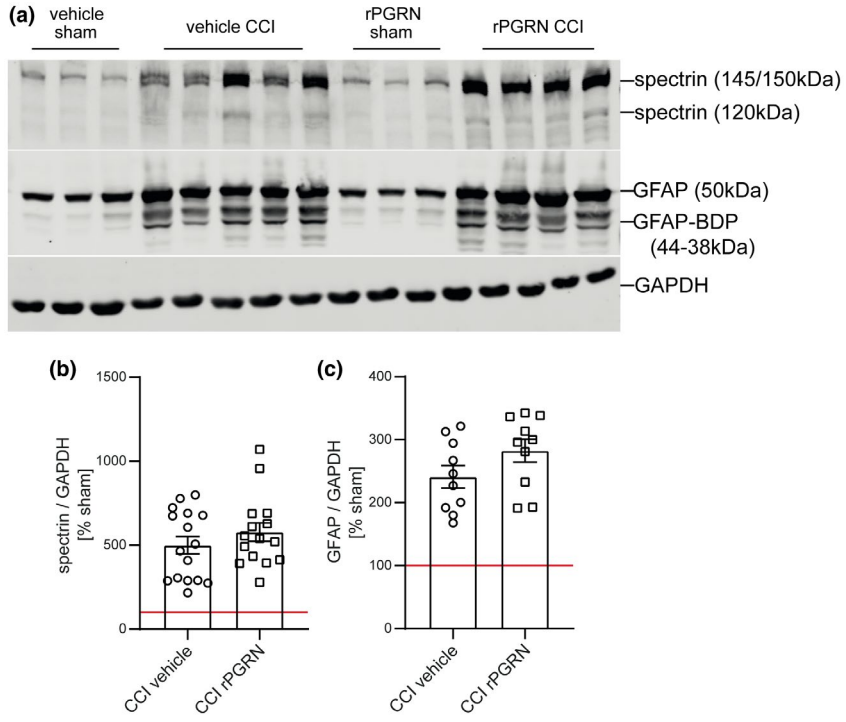

FIGURE 7 Neuronal injury and astrocyte activation are not influenced by recombinant progranulin (rPGRN). (a) Immunoblot showing spectrin and glial fibrillary acidic protein (GFAP) protein expression; glyceraldehyde 3-phosphate dehydrogenase (GAPDH) served as a reference (sham set to 100% = red line). (b) Quantification of breakdown products of spectrin. Sample size: vehicle controlled cortical impact (CCI): *n* (number of animals) = 16, rPGRN CCI *n* = 15. One significant outlier as determined by ROUT's test was removed from the rPGRN CCI group. (c) Quantification of GFAP protein levels. Sample size: vehicle CCI: *n* = 10, rPGRN CCI: *n* = 10. Data are expressed as mean ± *SEM*, and individual values are shown

but was not altered in rPGRN-treated CCI mice compared with sham (Figure 8c). Hence, in our TBI model, rPGRN did not protect the BBB but rather further impaired BBB integrity.

4 | DISCUSSION

The pleiotropic factor PGRN has wide-ranging functions in the periphery as well as in the central nervous system where its expression is confined to certain neuronal populations and activated microglia (Petkau & Leavitt, 2014). Its anti-inflammatory (Tang et al., 2011) and neurotrophic (Gass, Lee, et al., 2012) properties have been evaluated in various acute brain disorders and were predominantly interpreted as being beneficial. More recent studies, however suggest a possible negative effect of cleaved PGRN on cerebral inflammation and T-cell infiltration after brain injuries (Amado et al., 2019; Horinokita et al., 2019). As the pathophysiological roles of PGRN and cleaved granulins after brain injury have not yet been fully understood, the therapeutic value of rPGRN after experimental TBI is still unclear. It is of great importance to study putative positive and negative effects prior to development of PGRN-enhancing or supplementary treatments in the context of brain injuries (Chitramuthu et al., 2017; Gass et al., 2012). In this study, we assessed effects of an ICV injection of rPGRN immediately prior to experimental brain trauma for the acute phase after TBI. Neurological testing before (immuno)histochemical, mRNA, and protein analyses of the injured mouse brain at 5 dpi was carried out.

In contrast to the positive effects of rPGRN administration described by our and other laboratories (Egashira et al., 2013; Li et al., 2015; Menzel et al., 2017; Zhou et al., 2015), a single dose of rPGRN administered by ICV injection was not sufficient to attenuate the detrimental pro-inflammatory posttraumatic effects in our TBI model. The rescue effect of rPGRN in PGRN-deficient mice shown in our previous work may be explained by replacement of the missing PGRN, that is, restoration of the normal levels (Menzel et al., 2017).

In the present study, we unexpectedly observed that rPGRN-treated animals had an exacerbated BBB disruption. The maintenance of BBB functions is a major therapeutic goal, which is supposed to reduce the deleterious secondary effects of TBI (Jullienne & Badaut, 2013; Thal & Neuhaus, 2014). Expression of PGRN in the developing cerebral microvasculature indicates that a role in pathological conditions like FTD (Daniel et al., 2003; De Reuck et al., 2012) and PGRN has been reported to protect the BBB in an animal model of ischemic stroke (Kanazawa et al., 2015). However, here we found that rPGRN administration caused a further barrier breakdown evidenced by increased IgG extravasation into the perilesional brain tissue and nonoccurrence of the normal TBI-evoked counter-regulatory upregulation of the tight junction marker occludin. This is in contrast to studies in ischemic brain injury with PGRN-deficient mice showing an impaired ultrastructure of the BBB with alterations in endothelial tight junctions and increased hemorrhage (Jackman et al., 2013a). Furthermore, previously, PGRN at doses in the nanogram range improved neurological function and cerebral edema in subarachnoid hemorrhage in rats (Li et al., 2015; Zhou et al., 2015). Hence, the controversy may arise from differences in doses, treatment schedules, injury models, or animal species.

As mentioned, rPGRN is sufficient to rescue exaggerated injury and inflammation in PGRN-deficient mice in the CCI model of TBI (Menzel et al., 2017). Our data suggest that excess exogenous administration of rPGRN might lead to a ceiling effect and cannot further enhance its neuroprotective effects over baseline values. For example, inhibition of tumor necrosis factor alpha by rPGRN strongly depends

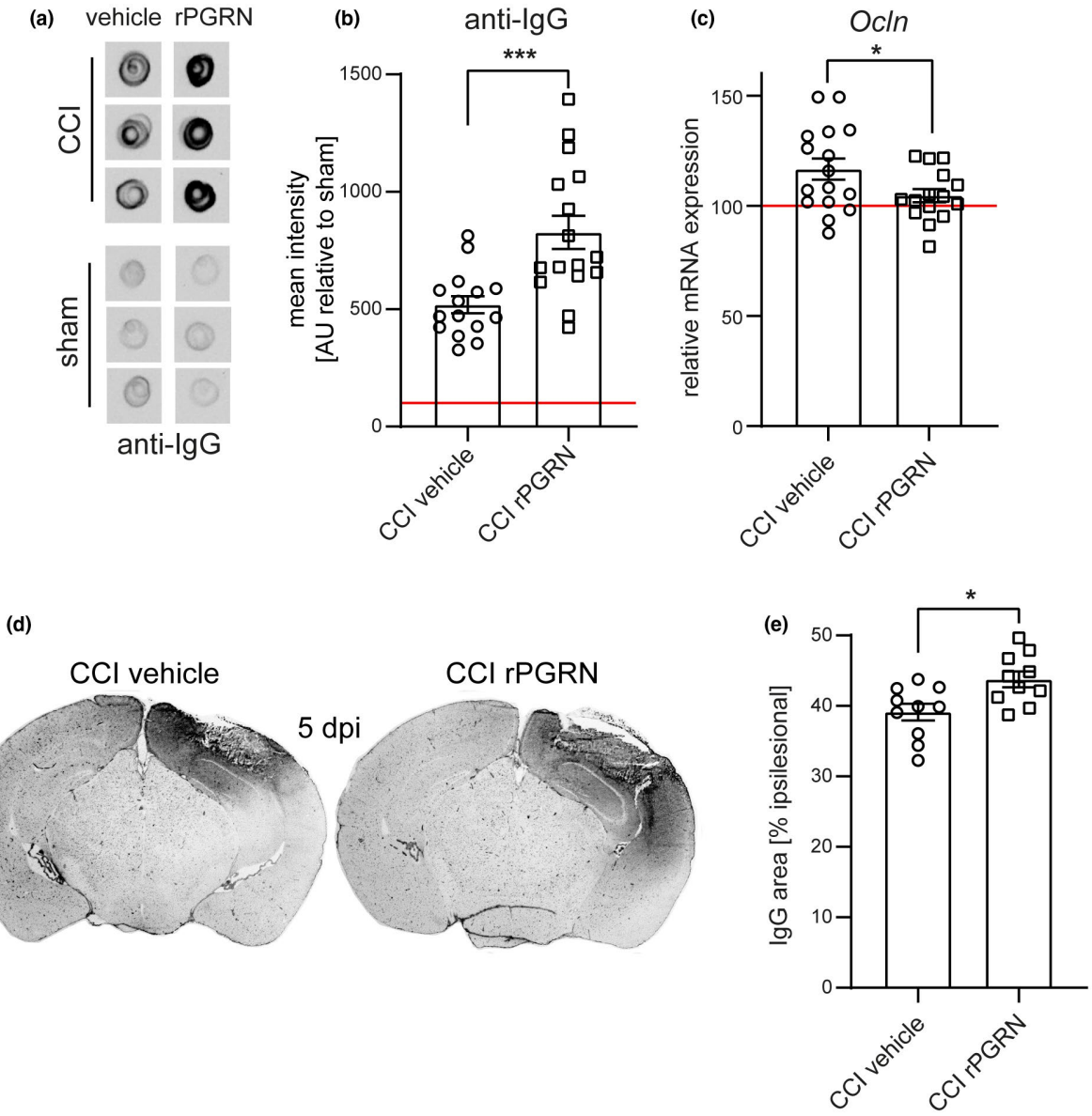

FIGURE 8 Recombinant progranulin (rPGRN) adversely affects the blood-brain barrier after traumatic brain injury. (a) Representative examples of immunodot blots to assess immunoglobulin G (IgG) extravasation in the lesioned hemisphere at 5 days post injury (dpi) (b) Quantification of IgG extravasation into brain tissue as arbitrary units (AU) relative to sham. Sample size: vehicle controlled cortical impact (CCI): *n* (number of animals) = 15, rPGRN CCI: *n* = 16. One significant outlier as determined by ROUT's test was removed from the vehicle CCI group. (c) Gene expression analyses of the tight junction marker occludin (*Ocln*), normalized to PPIA (sham set to 100% = red line). Sample size: vehicle CCI: *n* = 16, rPGRN CCI: *n* = 15. One significant outlier as determined by ROUT's test was removed from the rPGRN CCI group. (d) Histological staining of IgG in cryosections of vehicle- and rPGRN-treated CCI animals dpi. (e) Quantification of extravasation in % of the ipsilesional hemisphere. Sample size: vehicle CCI: *n* = 10, rPGRN CCI: *n* = 10. Data are expressed as mean ± *SEM* with individual values, and *p*-values were calculated by Student's unpaired *t*-test (*$p < .05$, ***$p < .001$ for differences between vehicle and rPGRN treatment)

on the number of TNF receptors on the cell surface. Once saturation of TNF receptor binding sites is reached, no further anti-inflammatory effects can be obtained from rPGRN (Tian et al., 2014). Consistent with this assumption, the histone deacetylase inhibitor suberoylanilide hydroxamic acid (SAHA) was only able to increase PGRN mRNA and protein levels in a dose-dependent manner up to a certain point (Cenik et al., 2011). These results support the idea that only certain levels of PGRN can be achieved or tolerated in vivo and higher concentrations cannot increase the neuroprotective effects of PGRN. This interpretation is also supported by the counter-regulatory decrease in endogenous PGRN mRNA expression in rPGRN-treated TBI mice.

The functional regulation of PGRN is complex because its biological activity is heavily dependent on proteolytic processing that leads to the release of small peptides (Bateman et al., 1990; Kao et al., 2017). On the one hand, full-length PGRN has anti-inflammatory and trophic activity, but, on the other hand, the proteolytic cleavage

products of PGRN, termed granulins, promote inflammatory activity (Cenik et al., 2012; Zhu et al., 2002). We analyzed gene expression of factors involved in PGRN proteolysis. MMP9 can cleave PGRN into granulin peptides extracellularly (Jawaid et al., 2009), the cysteine protease cathepsin L exerts its activity inside the lysosome after endosomal uptake of PGRN (Paushter et al., 2018), and Slpi inhibits PGRN cleavage in the extracellular compartment (Eriksen & Mackenzie, 2008). This tightly controlled balanced process of pro- and anti-proteolytic actions might be dysregulated under pathological conditions such as TBI. For instance, dysregulation of fibrinolysis with posttraumatic coagulation malfunction is a critical process in promoting secondary brain damage after murine and human TBI (Griemert et al., 2019; Hijazi et al., 2015). We found that the brain gene expression of the PGRN processing enzymes was markedly increased in CCI compared with sham animals, indicating a pathophysiological role in acute TBI. However, no difference was found between rPGRN- or vehicle-treated CCI animals.

Up to date, little is known about the biological processing of exogenously administered rPGRN. Cleavage by proteases can occur before the protein is taken up by the cells, and as a consequence, rPGRN has failed to exert its biological effects, but was possibly cleaved into granulin peptides, which then turn PGRN's putative benefit into the opposite, because these granulins evoked pro-inflammatory effects (Kessenbrock et al., 2008; Salazar et al., 2015). By inhibiting the production of granulins at early stages after cerebral ischemia via the administration of sivelestat, a specific neutrophil elastase inhibitor, neurological deficits in rats can be improved substantially (Horinokita et al., 2019). Therefore, rPGRN administration into a pro-inflammatory milieu with activated proteases might lead to a preferential increase in granulin levels rather than an accumulation of uncleaved PGRN, resulting in harmful effects. Hence, the time of injection may be critical, and further detailed studies into PGRN processing and granulin production are required.

Some limitations of our findings need to be taken into consideration. Sortilin is a protein expressed by neurons and mediates endocytosis and lysosomal localization of PGRN, thus decreasing the available amount of PGRN in the extracellular space (Hu et al., 2010). The rPGRN used in our study has a C-terminal 6-His tag that likely masks the sortilin interaction site (Zheng et al., 2011) and could lead to unphysiologically high PGRN levels in the perilesional brain parenchyma. Second, our open-skull TBI model requires craniotomy, which can be considered as a contributing factor to the injury (Cole et al., 2011). A third limiting aspect is our survival time point of 5 dpi. Shorter and longer observation times might shed further light on the effects of rPGRN, especially since opening of the BBB is an event occurring within hours after trauma (Cash & Theus, 2020).

Taken together, our study underscores the need for careful reflection and further studies focusing on the effects of PGRN and processing proteases, before considering PGRN supplementary or enhancing therapies for neurodegenerative disorders in clinical settings of brain injury.

ETHICS APPROVAL AND CONSENT TO PARTICIPATE

All experiments were conducted in compliance with the institutional guidelines of the Johannes Gutenberg University, Mainz, Germany, and approved by the Animal Care and Ethics Committee of the Landesuntersuchungsamt Rheinland-Pfalz (Tierversuchsantrag protocol number G12-1-052).

ACKNOWLEDGEMENTS

This study was supported by the Mainz Research School of Translational Biomedicine (TransMed), University Medical Center Johannes Gutenberg-University Mainz. We gratefully acknowledge the excellent technical assistance of Tobias Hirnet, Frida Kornes, and Dana Pieter (Department of Anesthesiology, Mainz, Germany). Data shown in this manuscript are part of the master thesis of SW and ML and the professional dissertation (Habilitation) of RH presented to the Faculty of Medicine of the Johannes Gutenberg-University Mainz.

All experiments were conducted in compliance with the ARRIVE guidelines.

CONFLICTS OF INTERESTS

All authors declare that there is no conflict of interest regarding the publication of this article and no competing financial interests exist.

AUTHORS' CONTRIBUTIONS

SW, ML, YW, CG, and RH performed experiments and collected data. MKES, IT, and RH conceived and designed experiments and analysis. MKES, CG, and RH performed data analysis. MKES, IT, and RH wrote the manuscript. All authors approved the final manuscript.

DATA AVAILABILITY STATEMENT

The datasets generated and analyzed during the current study are included in this published article or available from the authors upon reasonable request.

ORCID

Yong Wang https://orcid.org/0000-0001-6134-9079
Irmgard Tegeder https://orcid.org/0000-0001-7524-8025
Michael K. E. Schäfer https://orcid.org/0000-0001-6055-6244

REFERENCES

Almutairi, M. M., Gong, C., Xu, Y. G., Chang, Y., & Shi, H. (2016). Factors controlling permeability of the blood-brain barrier. *Cellular and Molecular Life Sciences: CMLS*, *73*, 57–77. https://doi.org/10.1007/s00018-015-2050-8

Altmann, C., Vasic, V., Hardt, S., Heidler, J., Häussler, A., Wittig, I., Schmidt, M. H. H., & Tegeder, I. (2016). Progranulin promotes peripheral nerve regeneration and reinnervation: Role of notch signaling. *Molecular Neurodegeneration*, *11*, 69. https://doi.org/10.1186/s13024-016-0132-1

Amado, D. A., Rieders, J. M., Diatta, F., Hernandez-Con, P., Singer, A., Mak, J. T., Zhang, J., Lancaster, E., Davidson, B. L., & Chen-Plotkin, A. S. (2019). AAV-mediated progranulin delivery to a mouse model of progranulin deficiency causes T cell-mediated toxicity. *Molecular Therapy*, *27*, 465–478. https://doi.org/10.1016/j.ymthe.2018.11.013

Asakura, R., Matsuwaki, T., Shim, J. H., Yamanouchi, K., & Nishihara, M. (2011). Involvement of progranulin in the enhancement of hippocampal neurogenesis by voluntary exercise. *NeuroReport*, *22*, 881–886. https://doi.org/10.1097/WNR.0b013e32834bf4ca

Bateman, A., Belcourt, D., Bennett, H., Lazure, C., & Solomon, S. (1990). Granulins, a novel class of peptide from leukocytes. *Biochemical and Biophysical Research Communications*, *173*, 1161–1168. https://doi.org/10.1016/S0006-291X(05)80908-8

Bateman, A., Cheung, S. T., & Bennett, H. P. J. (2018). A Brief overview of progranulin in health and disease. *Methods in Molecular Biology*, *1806*, 3–15.

Cash, A., & Theus, M. H. (2020). Mechanisms of blood-brain barrier dysfunction in traumatic brain injury. *International Journal of Molecular Sciences*, *21*, 3344. https://doi.org/10.3390/ijms21093344

Cenik, B., Sephton, C. F., Dewey, C. M., Xian, X., Wei, S., Yu, K., Niu, W., Coppola, G., Coughlin, S. E., Lee, S. E., Dries, D. R., Almeida, S., Geschwind, D. H., Gao, F.-B., Miller, B. L., Farese, R. V., Posner, B. A., Yu, G., & Herz, J. (2011). Suberoylanilide hydroxamic acid (vorinostat) up-regulates progranulin transcription: Rational therapeutic approach to frontotemporal dementia. *The Journal of Biological Chemistry*, *286*, 16101–16108. https://doi.org/10.1074/jbc.M110.193433

Cenik, B., Sephton, C. F., Kutluk Cenik, B., Herz, J., & Yu, G. (2012). Progranulin: A proteolytically processed protein at the crossroads of inflammation and neurodegeneration. *The Journal of Biological Chemistry*, *287*, 32298–32306. https://doi.org/10.1074/jbc.R112.399170

Chiba, Y., Danno, S., Suto, R., Suto, W., Yamane, Y., Hanazaki, M., Katayama, H., & Sakai, H. (2018). Intranasal administration of recombinant progranulin inhibits bronchial smooth muscle hyperresponsiveness in mouse allergic asthma. *American Journal of Physiology. Lung Cellular and Molecular Physiology*, *314*, L215–l223. https://doi.org/10.1152/ajplung.00575.2016

Chitramuthu, B. P., Bennett, H. P. J., & Bateman, A. (2017). Progranulin: A new avenue towards the understanding and treatment of neurodegenerative disease. *Brain: A Journal of Neurology*, *140*, 3081–3104.

Cole, J. T., Yarnell, A., Kean, W. S., Gold, E., Lewis, B., Ren, M., McMullen, D. C., Jacobowitz, D. M., Pollard, H. B., O'Neill, J. T., Grunberg, N. E., Dalgard, C. L., Frank, J. A., & Watson, W. D. (2011). Craniotomy: True sham for traumatic brain injury, or a sham of a sham? *Journal of Neurotrauma*, *28*, 359–369. https://doi.org/10.1089/neu.2010.1427

Crane, P. K., Gibbons, L. E., Dams-O'Connor, K., Trittschuh, E., Leverenz, J. B., Keene, C. D., Sonnen, J., Montine, T. J., Bennett, D. A., Leurgans, S., Schneider, J. A., & Larson, E. B. (2016). Association of traumatic brain injury with late-life neurodegenerative conditions and neuropathologic findings. *JAMA Neurology*, *73*, 1062–1069. https://doi.org/10.1001/jamaneurol.2016.1948

Daniel, R., Daniels, E., He, Z., & Bateman, A. (2003). Progranulin (acrogranin/PC cell-derived growth factor/granulin-epithelin precursor) is expressed in the placenta, epidermis, microvasculature, and brain during murine development. *Developmental Dynamics: An Official Publication of the American Association of Anatomists*, *227*, 593–599. https://doi.org/10.1002/dvdy.10341

Dash, P. K., Mach, S. A., & Moore, A. N. (2001). Enhanced neurogenesis in the rodent hippocampus following traumatic brain injury. *Journal of Neuroscience Research*, *63*, 313–319. https://doi.org/10.1002/1097-4547(20010215)63:4<313:AID-JNR1025>3.0.CO;2-4

De Reuck, J., Deramecourt, V., Cordonnier, C., Auger, F., Durieux, N., Bordet, R., Maurage, C. A., Leys, D., & Pasquier, F. (2012). Detection of microbleeds in post-mortem brains of patients with frontotemporal lobar degeneration: A 7.0-Tesla magnetic resonance imaging study with neuropathological correlates. *European Journal of Neurology*, *19*, 1355–1360. https://doi.org/10.1111/j.1468-1331.2012.03776.x

Egashira, Y., Suzuki, Y., Azuma, Y., Takagi, T., Mishiro, K., Sugitani, S., Tsuruma, K., Shimazawa, M., Yoshimura, S., Kashimata, M., Iwama, T., & Hara, H. (2013). The growth factor progranulin attenuates neuronal injury induced by cerebral ischemia-reperfusion through the suppression of neutrophil recruitment. *Journal of Neuroinflammation*, *10*, 105. https://doi.org/10.1186/1742-2094-10-105

Eriksen, J. L., & Mackenzie, I. R. (2008). Progranulin: Normal function and role in neurodegeneration. *Journal of Neurochemistry*, *104*, 287–297.

Faden, A. I., & Loane, D. J. (2015). Chronic neurodegeneration after traumatic brain injury: Alzheimer disease, chronic traumatic encephalopathy, or persistent neuroinflammation? *Neurotherapeutics: The Journal of the American Society for Experimental NeuroTherapeutics*, *12*, 143–150. https://doi.org/10.1007/s13311-014-0319-5

Gass, J., Lee, W. C., Cook, C., Finch, N., Stetler, C., Jansen-West, K., Lewis, J., Link, C. D., Rademakers, R., Nykjær, A., & Petrucelli, L. (2012). Progranulin regulates neuronal outgrowth independent of sortilin. *Molecular Neurodegeneration*, *7*, 33. https://doi.org/10.1186/1750-1326-7-33

Gass, J., Prudencio, M., Stetler, C., & Petrucelli, L. (2012). Progranulin: An emerging target for FTLD therapies. *Brain Research*, *1462*, 118–128. https://doi.org/10.1016/j.brainres.2012.01.047

Gölz, C., Kirchhoff, F. P., Westerhorstmann, J., Schmidt, M., Hirnet, T., Rune, G. M., Bender, R. A., & Schäfer, M. K. E. (2019). Sex hormones modulate pathogenic processes in experimental traumatic brain injury. *Journal of Neurochemistry*, *150*(2), 173–187. https://doi.org/10.1111/jnc.14678

Griemert, E.-V., Schwarzmaier, S. M., Hummel, R., Gölz, C., Yang, D., Neuhaus, W., Burek, M., Förster, C. Y., Petkovic, I., Trabold, R., Plesnila, N., Engelhard, K., Schäfer, M. K., & Thal, S. C. (2019). Plasminogen activator inhibitor-1 augments damage by impairing fibrinolysis after traumatic brain injury. *Annals of Neurology*, *85*, 667–680. https://doi.org/10.1002/ana.25458

Hay, J. R., Johnson, V. E., Young, A. M., Smith, D. H., & Stewart, W. (2015). Blood-brain barrier disruption is an early event that may persist for many years after traumatic brain injury in humans. *Journal of Neuropathology and Experimental Neurology*, *74*, 1147–1157.

Hijazi, N., Abu Fanne, R., Abramovitch, R., Yarovoi, S., Higazi, M., Abdeen, S., Basheer, M., Maraga, E., Cines, D. B., & Al-Roof Higazi, A. (2015). Endogenous plasminogen activators mediate progressive intracerebral hemorrhage after traumatic brain injury in mice. *Blood*, *125*, 2558–2567. https://doi.org/10.1182/blood-2014-08-588442

Horinokita, I., Hayashi, H., Oteki, R., Mizumura, R., Yamaguchi, T., Usui, A., Yuan, B., & Takagi, N. (2019). Involvement of progranulin and granulin expression in inflammatory responses after cerebral ischemia. *International Journal of Molecular Sciences*, *20*. https://doi.org/10.3390/ijms20205210

Hsiung, G. Y. R., & Feldman, H. H. (1993). GRN frontotemporal dementia. In M. P. Adam, H. H. Ardinger, R. A. Pagon, S. E. Wallace, L. J. H. Bean, K. Stephens, & A. Amemiya (Eds.), *GeneReviews((R))*. University of Washington.

Hu, F., Padukkavidana, T., Vaegter, C. B., Brady, O. A., Zheng, Y., Mackenzie, I. R., Feldman, H. H., Nykjaer, A., & Strittmatter, S. M. (2010). Sortilin-mediated endocytosis determines levels of the frontotemporal dementia protein, progranulin. *Neuron*, *68*, 654–667. https://doi.org/10.1016/j.neuron.2010.09.034

Huang, C., Sakry, D., Menzel, L., Dangel, L., Sebastiani, A., Krämer, T., Karram, K., Engelhard, K., Trotter, J., & Schäfer, M. K. E. (2016). Lack of NG2 exacerbates neurological outcome and modulates glial responses after traumatic brain injury. *Glia*, *64*, 507–523. https://doi.org/10.1002/glia.22944

Hummel, R., Ulbrich, S., Appel, D., Li, S., Hirnet, T., Zander, S., Bobkiewicz, W., Gölz, C., & Schäfer, M. K. E. (2020). Administration of all-trans retinoic acid after experimental traumatic brain injury is brain protective. *British Journal of Pharmacology*, *177*, 5208–5223.

Jackman, K., Kahles, T., Lane, D., Garcia-Bonilla, L., Abe, T., Capone, C., Hochrainer, K., Voss, H., Zhou, P., Ding, A., Anrather, J., & Iadecola, C. (2013a). Progranulin deficiency promotes post-ischemic blood-brain barrier disruption. *The Journal of Neuroscience: The Official Journal of the Society for Neuroscience*, *33*, 19579–19589. https://doi.org/10.1523/JNEUROSCI.4318-13.2013

Jackman, K., Kahles, T., Lane, D., Garcia-Bonilla, L., Abe, T., Capone, C., Hochrainer, K., Voss, H., Zhou, P., Ding, A., Anrather, J., & Iadecola, C. (2013b). Progranulin deficiency promotes post-ischemic blood-brain barrier disruption. *The Journal of Neuroscience: The Official Journal of the Society for Neuroscience*, *33*, 19579–19589. https://doi.org/10.1523/JNEUROSCI.4318-13.2013

Jawaid, A., Rademakers, R., Kass, J. S., Kalkonde, Y., & Schulz, P. E. (2009). Traumatic brain injury may increase the risk for frontotemporal dementia through reduced progranulin. *Neuro-degenerative Diseases*, *6*, 219–220. https://doi.org/10.1159/000258704

Jiao, H., Wang, Z., Liu, Y., Wang, P., & Xue, Y. (2011). Specific role of tight junction proteins claudin-5, occludin, and ZO-1 of the blood-brain barrier in a focal cerebral ischemic insult. *Journal of Molecular Neuroscience : MN*, *44*, 130–139. https://doi.org/10.1007/s12031-011-9496-4

Johnson, V. E., Stewart, W., & Smith, D. H. (2013). Axonal pathology in traumatic brain injury. *Experimental Neurology*, *246*, 35–43. https://doi.org/10.1016/j.expneurol.2012.01.013

Jullienne, A., & Badaut, J. (2013). Molecular contributions to neurovascular unit dysfunctions after brain injuries: Lessons for target-specific drug development. *Future Neurology*, *8*, 677–689. https://doi.org/10.2217/fnl.13.55

Kanazawa, M., Kawamura, K., Takahashi, T., Miura, M., Tanaka, Y., Koyama, M., Toriyabe, M., Igarashi, H., Nakada, T., Nishihara, M., Nishizawa, M., & Shimohata, T. (2015). Multiple therapeutic effects of progranulin on experimental acute ischaemic stroke. *Brain: A Journal of Neurology*, *138*, 1932–1948. https://doi.org/10.1093/brain/awv079

Kao, A. W., McKay, A., Singh, P. P., Brunet, A., & Huang, E. J. (2017). Progranulin, lysosomal regulation and neurodegenerative disease. *Nature Reviews Neuroscience*, *18*, 325–333. https://doi.org/10.1038/nrn.2017.36

Kessenbrock, K., Fröhlich, L., Sixt, M., Lämmermann, T., Pfister, H., Bateman, A., Belaaouaj, A., Ring, J., Ollert, M., Fässler, R., & Jenne, D. E. (2008). Proteinase 3 and neutrophil elastase enhance inflammation in mice by inactivating antiinflammatory progranulin. *The Journal of Clinical Investigation*, *118*, 2438–2447. https://doi.org/10.1172/JCI34694

Krämer, T., Grob, T., Menzel, L., Hirnet, T., Griemert, E., Radyushkin, K., Thal, S. C., Methner, A., & Schäfer, M. K. E. (2017). Dimethyl fumarate treatment after traumatic brain injury prevents depletion of antioxidative brain glutathione and confers neuroprotection. *Journal of Neurochemistry*, *143*, 523–533. https://doi.org/10.1111/jnc.14220

Lau, T. T., Zhang, F., Tang, W., & Wang, D. A. (2016). Release of transgenic progranulin from a living hyaline cartilage graft model: An in vitro evaluation on anti-inflammation. *Journal of Biomedical Materials Research Part A*, *104*, 2968–2977.

Li, B., He, Y., Xu, L., Hu, Q., Tang, J., Chen, Y., Tang, J., Feng, H., & Zhang, J. H. (2015). Progranulin reduced neuronal cell death by activation of sortilin 1 signaling pathways after subarachnoid hemorrhage in rats. *Critical Care Medicine*, *43*, e304–311. https://doi.org/10.1097/CCM.0000000000001096

Li, X., Cheng, S., Hu, H., Zhang, X., Xu, J., Wang, R., & Zhang, P. (2020). Progranulin protects against cerebral ischemia-reperfusion (I/R) injury by inhibiting necroptosis and oxidative stress. *Biochemical and Biophysical Research Communications*, *521*, 569–576. https://doi.org/10.1016/j.bbrc.2019.09.111

LoBue, C., Wilmoth, K., Cullum, C. M., Rossetti, H. C., Lacritz, L. H., Hynan, L. S., Hart, J. Jr, & Womack, K. B. (2016). Traumatic brain injury history is associated with earlier age of onset of frontotemporal dementia. *Journal of Neurology, Neurosurgery, and Psychiatry*, *87*, 817–820.

Ma, Y., Matsuwaki, T., Yamanouchi, K., & Nishihara, M. (2017). Progranulin protects hippocampal neurogenesis via suppression of neuroinflammatory responses under acute immune stress. *Molecular Neurobiology*, *54*, 3717–3728. https://doi.org/10.1007/s12035-016-9939-6

Menzel, L., Kleber, L., Friedrich, C., Hummel, R., Dangel, L., Winter, J., Schmitz, K., Tegeder, I., & Schafer, M. K. (2017). Progranulin protects against exaggerated axonal injury and astrogliosis following traumatic brain injury. *Glia*, *65*, 278–292. https://doi.org/10.1002/glia.23091

Newcomb, J. K., Kampfl, A., Posmantur, R. M., Zhao, X., Pike, B. R., Liu, S. J., Clifton, G. L., & Hayes, R. L. (1997). Immunohistochemical study of calpain-mediated breakdown products to alpha-spectrin following controlled cortical impact injury in the rat. *Journal of Neurotrauma*, *14*, 369–383.

Paushter, D. H., Du, H., Feng, T., & Hu, F. (2018). The lysosomal function of progranulin, a guardian against neurodegeneration. *Acta Neuropathologica*, *136*, 1–17. https://doi.org/10.1007/s00401-018-1861-8

Petkau, T. L., & Leavitt, B. R. (2014). Progranulin in neurodegenerative disease. *Trends in Neurosciences*, *37*, 388–398. https://doi.org/10.1016/j.tins.2014.04.003

Petkau, T. L., Neal, S. J., Orban, P. C., MacDonald, J. L., Hill, A. M., Lu, G., Feldman, H. H., Mackenzie, I. R., & Leavitt, B. R. (2010). Progranulin expression in the developing and adult murine brain. *The Journal of Comparative Neurology*, *518*, 3931–3947. https://doi.org/10.1002/cne.22430

Salazar, D. A., Butler, V. J., Argouarch, A. R., Hsu, T.-Y., Mason, A., Nakamura, A., McCurdy, H., Cox, D., Ng, R., Pan, G., Seeley, W. W., Miller, B. L., & Kao, A. W. (2015). The progranulin cleavage products, granulins, exacerbate TDP-43 toxicity and increase TDP-43 levels. *The Journal of Neuroscience: The Official Journal of the Society for Neuroscience*, *35*, 9315–9328. https://doi.org/10.1523/JNEUROSCI.4808-14.2015

Schäfer, M. K. E., & Tegeder, I. (2018). NG2/CSPG4 and progranulin in the posttraumatic glial scar. *Matrix Biology: Journal of the International Society for Matrix Biology*, *68–69*, 571–588. https://doi.org/10.1016/j.matbio.2017.10.002

Schaible, E. V., Windschugl, J., Bobkiewicz, W., Kaburov, Y., Dangel, L., Krämer, T., Huang, C., Sebastiani, A., Luh, C., Werner, C., & Engelhard, K. (2014). 2-Methoxyestradiol confers neuroprotection and inhibits a maladaptive HIF-1alpha response after traumatic brain injury in mice. *Journal of Neurochemistry*, *129*, 940–954.

Schildge, S., Bohrer, C., Beck, K., & Schachtrup, C. (2013). Isolation and culture of mouse cortical astrocytes. *Journal of Visualized Experiments: Jove*. https://doi.org/10.3791/50079

Schober, M. E., Requena, D. F., Davis, L. J., Metzger, R. R., Bennett, K. S., Morita, D., Niedzwecki, C., Yang, Z., & Wang, K. K. (2014). Alpha II Spectrin breakdown products in immature Sprague Dawley rat hippocampus and cortex after traumatic brain injury. *Brain Research*, *1574*, 105–112. https://doi.org/10.1016/j.brainres.2014.05.046

Scott, G., Zetterberg, H., Jolly, A., Cole, J. H., De Simoni, S., Jenkins, P. O., Feeney, C., Owen, D. R., Lingford-Hughes, A., Howes, O., Patel, M. C., Goldstone, A. P., Gunn, R. N., Blennow, K., Matthews, P. M., & Sharp, D. J. (2018). Minocycline reduces chronic microglial activation after brain trauma but increases neurodegeneration. *Brain: A Journal of Neurology*, *141*, 459–471. https://doi.org/10.1093/brain/awx339

Staib-Lasarzik, I., Nagel, N., Sebastiani, A., Griemert, E. V., & Thal, S. C. (2019). Analgesic treatment limits surrogate parameters for early stress and pain response after experimental subarachnoid hemorrhage. *BMC Neuroscience*, *20*, 49. https://doi.org/10.1186/s12868-019-0531-7

Stocchetti, N., & Zanier, E. R. (2016). Chronic impact of traumatic brain injury on outcome and quality of life: A narrative review. *Critical Care (London, England)*, *20*, 148. https://doi.org/10.1186/s13054-016-1318-1

Tanaka, Y., Chambers, J. K., Matsuwaki, T., Yamanouchi, K., & Nishihara, M. (2014). Possible involvement of lysosomal dysfunction in pathological changes of the brain in aged progranulin-deficient mice. *Acta Neuropathologica Communications*, *2*, 78. https://doi.org/10.1186/s40478-014-0078-x

Tanaka, Y., Matsuwaki, T., Yamanouchi, K., & Nishihara, M. (2013). Exacerbated inflammatory responses related to activated microglia after traumatic brain injury in progranulin-deficient mice. *Neuroscience*, *231*, 49–60. https://doi.org/10.1016/j.neuroscience.2012.11.032

Tang, W., Lu, Y., Tian, Q. Y., Zhang, Y., Guo, F. J., Liu, G. Y., Syed, N. M., Lai, Y., Lin, E. A., Kong, L., & Su, J. (2011). The growth factor progranulin binds to TNF receptors and is therapeutic against inflammatory arthritis in mice. *Science*, *332*, 478–484.

Tao, J., Ji, F., Wang, F., Liu, B., & Zhu, Y. (2012). Neuroprotective effects of progranulin in ischemic mice. *Brain Research*, *1436*, 130–136. https://doi.org/10.1016/j.brainres.2011.11.063

Thal, S. C., & Neuhaus, W. (2014). The blood-brain barrier as a target in traumatic brain injury treatment. *Archives of Medical Research*, *45*, 698–710. https://doi.org/10.1016/j.arcmed.2014.11.006

Thal, S. C., Wyschkon, S., Pieter, D., Engelhard, K., & Werner, C. (2008). Selection of endogenous control genes for normalization of gene expression analysis after experimental brain trauma in mice. *Journal of Neurotrauma*, *25*, 785–794. https://doi.org/10.1089/neu.2007.0497

Tian, Q., Zhao, Y., Mundra, J. J., Gonzalez-Gugel, E., Jian, J., Uddin, S. M., & Liu, C. (2014). Three TNFR-binding domains of PGRN act independently in inhibition of TNF-alpha binding and activity. *Frontiers in Bioscience (Landmark edition)*, *19*, 1176–1185. https://doi.org/10.2741/4274

Timaru-Kast, R., Luh, C., Gotthardt, P., Huang, C., Schäfer, M. K., Engelhard, K., & Thal, S. C. (2012). Influence of age on brain edema formation, secondary brain damage and inflammatory response after brain trauma in mice. *PLoS One*, *7*, e43829. https://doi.org/10.1371/journal.pone.0043829

Wang, C., Zhang, L., Ndong, J. C., Hettinghouse, A., Sun, G., Chen, C., Zhang, C., Liu, R., & Liu, C. J. (2019). Progranulin deficiency exacerbates spinal cord injury by promoting neuroinflammation and cell apoptosis in mice. *Journal of Neuroinflammation*, *16*, 238. https://doi.org/10.1186/s12974-019-1630-1

Wang, X., Gao, X., Michalski, S., Zhao, S., & Chen, J. (2016). Traumatic brain injury severity affects neurogenesis in adult mouse hippocampus. *Journal of Neurotrauma*, *33*, 721–733. https://doi.org/10.1089/neu.2015.4097

Wen, J., Qian, S., Yang, Q., Deng, L., Mo, Y., & Yu, Y. (2014). Overexpression of netrin-1 increases the expression of tight junction-associated proteins, claudin-5, occludin, and ZO-1, following traumatic brain injury in rats. *Experimental and Therapeutic Medicine*, *8*, 881–886. https://doi.org/10.3892/etm.2014.1818

Zheng, Y., Brady, O. A., Meng, P. S., Mao, Y., & Hu, F. (2011). C-terminus of progranulin interacts with the beta-propeller region of sortilin to regulate progranulin trafficking. *PLoS One*, *6*, e21023. https://doi.org/10.1371/journal.pone.0021023

Zhou, C., Xie, G., Wang, C., Zhang, Z., Chen, Q., Zhang, L. I., Wu, L., Wei, Y., Ding, H., Hang, C., Zhou, M., & Shi, J. (2015). Decreased progranulin levels in patients and rats with subarachnoid hemorrhage: A potential role in inhibiting inflammation by suppressing neutrophil recruitment. *Journal of Neuroinflammation*, *12*, 200. https://doi.org/10.1186/s12974-015-0415-4

Zhou, Y., Shao, A., Yao, Y., Tu, S., Deng, Y., & Zhang, J. (2020). Dual roles of astrocytes in plasticity and reconstruction after traumatic brain injury. *Cell Communication and Signaling*, *18*, 62. https://doi.org/10.1186/s12964-020-00549-2

Zhu, J., Nathan, C., Jin, W., Sim, D., Ashcroft, G. S., Wahl, S. M., Lacomis, L., Erdjument-Bromage, H., Tempst, P., Wright, C. D., & Ding, A. (2002). Conversion of proepithelin to epithelins: Roles of SLPI and elastase in host defense and wound repair. *Cell*, *111*, 867–878. https://doi.org/10.1016/S0092-8674(02)01141-8

SUPPORTING INFORMATION

Additional supporting information may be found online in the Supporting Information section.

How to cite this article: Hummel R, Lang M, Walderbach S, et al. Single intracerebroventricular progranulin injection adversely affects the blood–brain barrier in experimental traumatic brain injury. *J Neurochem*. 2021;158:342–357. https://doi.org/10.1111/jnc.15375